SCIENTIFIC COMMITTEE
THIRTEENTH REGULAR SESSION

Rarotonga, Cook Islands
9-17 August 2017

Modelling the impact of climate change including ocean acidification on Pacific yellowfin tuna

---

WCPFC-SC13-2017/EB-WP-01

Patrick Lehodey[1], Inna Senina[1], Beatriz Calmettes[1], Morgane Dessert[2], Simon Nicol[3], John Hampton[3], Neville Smith[3], Thomas Gorgues4, Olivier Aumont[2], Matthieu Lengaigne[4], Christophe Menkes[4], and Marion Gehlen[5]

[1] Oceanic 1 Collecte Localisation Satellites (CLS), 11 rue Hermes, 31520 Ramonville St Agne, France
[2] IRD, LPO, IUEM Technopôle Brest-Iroise - rue Dumont d'Urville, 29280 Plouzané, France
[3] Oceanic Fisheries Programme (OFP), Pacific Community (SPC), B.P. D5, 98848 Nouméa, New Caledonia
[4] LOCEAN (Université Sorbonne - Pierre et Marie Curie, IRD/CNRS/MNHN) IRD, BP A5 98848 Nouméa Cedex, New Caledonia
[5] LSCE/IPSL, UMR CEA-CNRS-UVSQ, CEA Saclay, 91191 Gif-sur-Yvette cedex, Franc

Executive summary

- The effects on the ocean pelagic ecosystem, especially tuna resources, of ocean acidification and climate change are poorly known. This research presents an update of the previous yellowfin tuna SEAPODYM model (the last reference SEAPODYM model for Pacific yellowfin tuna was presented in 2015).
- SEAPODYM is a useful modelling framework to investigate the impact of climate changes on tuna populations. It integrates key relationships between fish population dynamics and the environmental conditions of their marine ecosystem in a spatially explicit representation, with a robust estimation approach of population dynamics and fisheries parameters.
- Elements of the yellowfin model which have been improved include additional fisheries catch data, the incorporation of enhanced multi-climate model approaches to projecting climate impacts, and an approach to quantify the plausible impacts of ocean acidification on yellowfin tuna, based on laboratory experiments. Critically for managers this paper presents novel projections of potential impacts arising from a range of ocean warming scenarios, and the likely compounding effects of concurrent ocean acidification.
- The new reference model provides a better fit to catch data. It is characterized by changes in the thermal habitats both for spawning and feeding yellowfin. The larval distribution is more strongly contrasted between areas than previously, with less dense concentrations in the central equatorial but higher densities in the eastern and western regions. There is increased convergence with MULTIFAN-CL biomass estimates, especially in the main fishing grounds in the tropical regions.
- The fishing impact over the historical period is predicted to have reduced the spawning biomass by an average of 35% in 2010 in the whole Pacific with much higher impact (>50%) in the equatorial eastern and western Pacific.
- This new reference solution, without fishing impact, provides initial population conditions and model parameterization for the climate change projections, under the IPCC RCP8.5 ("Business as usual") scenario, and with atmospheric forcings from five different Earth Climate models. Three additional runs for each forcing simulate low, medium and high sensitivity of larval stage to ocean acidification. Thus, the ensemble simulation has 20 members in total.
- The predicted impact of climate change on this yellowfin tuna population is mainly driven by the change in the spawning habitat (temperature and productivity) and subsequent larval recruitment with a decrease in the WCPO and increase in the EPO.
- The additional impact of ocean acidification is minor. There is no discernible impact when considering the low sensitivity scenario, very small effects (>5%) by the end of the century in the eastern equatorial Pacific ocean with the intermediate scenario S1 and a stronger negative impact reaching locally -10% in 2050 and -15% in 2100 with the high sensitivity scenario.
- The temporal trends in larval biomass predicted by all simulations are relatively stable in the WCPO until 2050 and start to decrease in the second half of the century, while the range of model responses widens after the 2060s.

- In the WCPO, three periods can be isolated. Until 2050, there is no detectable impact outside of natural variability. After a rapid shift around 2050, a second regime of lower productivity is maintained until 2080. Finally, the end of the time series is marked by one more decline in productivity with a wider range of uncertainty.
- In 2050, the most obvious changes relative to the first decade of the century are a large increase of unfished biomass in the ETPO (+37% on average) and a moderate decrease in the WTPO (-14% on average).
- The new ensemble approach appears robust as there is not one single or couple of models dominating the average trends, nor are trends observed with any model changing in parallel with another over time.
- This general framework can be now used to project the impact of fishing that remains the major external driver of the tuna population dynamics. While we used to apply a simple scenario relying on the mean fishing effort observed over recent years, it would be useful to develop alternative scenarios with sustainable long term objectives proposed by the WCPFC Scientific Committee.

Introduction

Since the beginning of industrial era, human fossil fuel combustion has released large amounts of CO2 into the atmosphere, which with other greenhouse gases, lead to the Earth climate warming. The ocean is absorbing a large quantity of this additional atmospheric CO2 derived from anthropogenic activity, thus slowing down the warming (greenhouse) effect. The direct impact is that the oceans are warming. However, the increased CO2 absorption by the ocean is also shifting the oceans carbonate chemical equilibrium towards a lower pH, i.e. more acidic waters and lower calcium carbonate saturation states (e.g. Caldeira and Wickett 2003; Feely et al. 2004; Barnett et al. 2005). These chemical changes are going to impact many calcifying species, e.g., shell-forming marine organisms. Ocean acidification will also likely impact non-calcifying species, e.g. through physiology and respiration (Pörtner et al. 2014). The effects on organisms and populations, and the consequences at the ecosystem level are largely unknown. Our knowledge is particularly limited for the ocean pelagic ecosystem, and this represents a significant challenge to fishery resource managers and policy-makers, who need to account for climate change and ocean acidification in addition to the strong fishing pressure on fish stocks, including the valuable tuna species.

The first studies investigating the impact of climate warming on Pacific tuna stocks have included changes in water temperature, currents, ocean productivity and dissolved oxygen (Lehodey et al. 2010, 2011, 2013, 2015; Bell et al. 2013). They have shown various likely responses of tuna species, usually driven by the impact of changes on the favourability of present spawning grounds. The core habitat of most tropical tuna species such as skipjack and yellowfin are predicted to shift from western to central and eastern equatorial Pacific, while the more temperate albacore tuna would likely see their spawning grounds shift poleward from tropical to subtropical waters after a declining phase of the present spawning grounds until the warming of subtropical waters reaches the optimal spawning temperature for this species. With the recent information and findings on the potential impact that ocean acidification could have on fish, and especially on tuna larvae (Pörtner 2014; Bromhead et al. 2015), it is necessary to assess its potential impact together with the other climate change effects. An international workshop was held in January 2016 to discuss these issues and define the best approach to assess the additional risk on tuna stocks due to ocean acidification (Nicol et al. 2016).

The workshop reviewed the state of knowledge on the impacts of ocean acidification on marine fishes (Nicol et al. 2016). It highlighted the great variability of impacts from species to species with some support evidence of increasing mortality of eggs and larvae with very high levels of pCO_2 (Baumann et al. 2012; Chambers et al. 2014), behavioural changes and sub-lethal effects such as tissue damage (Frommel et al. 2016), and also mechanisms of acclimation (Miller et al. 2012; Murray et al. 2014). It was also noted that pCO_2 levels in the central and eastern equatorial Pacific Ocean are projected to exceed 1000 µatm by 2080, which is a major concern for Pacific tuna fisheries as the core distributions for bigeye, skipjack, and yellowfin tuna are predicted to shift to this region between 2050 and 2100.

There was a consensus on the need to focus on the egg and larval stage of tuna which are the life stages most sensitive to ocean acidification. One first pilot study (Bromhead et al. 2015) that examined the potential impacts of ocean acidification on the eggs and larvae of yellowfin tuna provided some inconsistency in results, though it was relatively clear that ocean acidification effects on larvae were not evident until pCO_2 levels reached above 1500 µatm. A second study based on yellowfin larvae showed the detrimental effects of increased pCO2 through histological analyses of organs at levels at which significant effects on survival were not yet apparent (Frommel et al. 2016). Therefore, introducing an additional mechanism in the model SEAPODYM to test the impact of additional mortality on tuna larvae due to ocean acidification was seen as a priority. This report provides the method developed to include ocean acidification impact in the future trends of Pacific yellowfin tuna population under climate change projections with SEAPODYM. The method uses results from the first laboratory studies on yellowfin tuna, the results of the 2016 workshop, and also the ensemble simulation approach proposed to account for uncertainty in each single Earth Climate model projection (Nicol et al. 2014).

Method

SEAPODYM

The modelling approach of SEAPODYM has been extensively described in previous working documents of the WCPFC and in the scientific literature (e.g., Lehodey 2003, 2004, 2008; Senina et al. 2008, 2016). Unlike standard assessment model like MULTIFAN-CL or Stock Synthesis, the SEAPODYM model equations describe fish population dynamic processes (spawning, recruitment, movement, mortality) based on environmental functional relationships with temperature, dissolved oxygen concentration and distributions of prey (micronektonic tuna forage). The model simulates tuna age-structured population dynamics with different life stages. At larvae and juvenile phases, fish drift with currents; later on they become autonomous, i.e., in addition to the currents velocities their movement has additional component linked to their size and the habitat quality, as well as oceanic currents. The model takes into account fishing and predicts total catch and size frequencies of catch by fishery. The spatial dynamics, relying on advection-diffusion-reaction equations is fully-explicit, meaning that density of fish cohorts and catch are computed in each cell of a grid defined for the model domain. The Maximum Likelihood Estimation approach developed for SEAPODYM (Senina et al 2008) takes advantage of this spatially explicit representation by using the numerous (>> 100,000) catch/effort and length frequencies of catch data available at these resolutions.

The necessary input variables to run SEAPODYM are 3D (0~1000m depth) water temperature and currents, dissolved oxygen concentrations, total vertically-integrated primary production and euphotic depths. They are provided by the NEMO-PISCES coupled model (which requires environmental forcings for the historical period and the climate change projections, determined independently). The additional fields of pH needed for this study are also standard outputs of the PISCES model (Aumont et al. 2015).

Environmental forcings

Historical period

Rebuilding the past history of the tuna population under the combined effects of fishing pressure and natural climate variability (e.g., ENSO) is the first step to provide the most realistic initial conditions to start the projections under climate change scenarios. Physical (temperature and currents) and biogeochemical (primary production, euphotic depth and dissolved oxygen concentration) forcing variables for this historical period are provided by the ocean model NEMO (www.nemo-ocean.eu/) coupled to the biogeochemical model PISCES (Pelagic Interaction Scheme for Carbon and Ecosystem Studies; Aumont et al. 2015). The ocean physical model is driven by the ERA40-INTERIM (1972- 2011) atmospheric reanalysis (atmospheric temperature, zonal and meridional wind speeds, radiative heat fluxes, relative humidity, and precipitation) which has been corrected using satellite data (Dee et al. 2011). All forcing variables are interpolated on the same regular grid and same time step prior to use in SEAPODYM simulations. This physical-biogeochemical forcing is used first to simulate the zooplankton and micronekton functional groups (Lehodey et al. 2010a; 2015). Then, optimization experiments are conducted with a historical fishing dataset from the Pacific Ocean to obtain optimal parameterization of the model using the Maximum Likelihood Estimation (MLE) approach implemented with SEAPODYM (Senina et al., 2008; 2015; 2016).

Climate change projections

The previous studies modelling climate change impacts on tuna stocks with SEAPODYM have shown that Earth Climate models have their own biases and errors that can propagate critical biases in the projections of tuna populations (e.g., Lehodey et al. 2013). In the conclusion of these earlier SEAPODYM studies, it was proposed to run ensemble simulations to account for the uncertainty in model forcings, with an envelope of projections rather than a single projection. However, to avoid time consuming task of revising the model optimization over historical period of each Earth Climate model run, the approach considered was to achieve a single optimal solution derived from the best possible historical reanalysis (hindcast), and then to project this solution into the future, but using reconstructed forcings made of the sum of the historical mean state and the anomaly of the projection for each atmospheric variable (Nicol et al. 2014). The Nicol et al.(2014) approach has the advantage of searching for one single and best optimal solution over the historical period, and to have all future projections consistent with the historical period since they share the same mean state.

Atmospheric variables (atmospheric temperature, zonal and meridionnal wind speeds, radiative heat fluxes, relative humidity, and precipitation) generated by climate change simulations from five different Earth Climate models were obtained from the Coupled Model Intercomparison Project Phase 5 (CMIP5). The models selected were those that captured cycles similar to El Niño Southern Oscillation (ENSO) in their simulations (Bellenger et al., 2013, Table 1). The scenario used is the RCP8.5 (business as usual) as defined by IPCC for the 5th assessment exercise. Anomalies have been constructed from each Earth Climate model variable by subtracting the monthly climatology computed over the historical period (1979-2010). Therefore, the mean state is constrained by the historical reanalysis, whereas the short to long-term variability is derived from the Earth Climate models and includes climate change projections. Once processed the atmospheric forcings are used to drive the same coupled NEMO-PISCES ocean-biogeochemical model used for the historical period.

Table 1: Earth Climate models from which atmospheric variables have been used to run NEMO-PISCES coupled physical-biogeochemical model that provides input variables to SEAPODYM.

CMIP5 model name	Model / Modelling Centre
IPSL-CM5A-MR	IPSL (Institut Pierre Simon Laplace, France)
MIROC-ESM	MIROC (Model for Interdisciplinary Research on Climate, Japan)
NorESM1-ME	NorESM (Norwegian Climate Centre, Norway)
MPI-ESM-MR	MPI (Max Planck Institute for Meteorology, Germany)
GFDL-ESM2G	GFDL (Geophysical Fluid Dynamics Laboratory, USA)

Yellowfin tuna climate change projections with SEAPODYM

Reference SEAPODYM application to yellowfin tuna

The optimal solution of SEAPODYM for Pacific yellowfin tuna is numerically solved on a 2° regular grid at monthly time step. The age structure of yellowfin is discretized between 0 and age_{max} = 10 (yr) into monthly cohorts for the first five years and a latest cohort aggregating oldest individuals. Age-length and age-weight relationships were derived from the MULTIFAN-CL estimate (Langley et al 2011). The species is assumed to be opportunistic spawner with a spawning success proportional to the spawning habitat index and the larvae stock-recruitment (Beverton and Holt) function computed locally at the cell level. The initial conditions at the beginning of the simulation (1979) were obtained using the previous reference configuration (Senina et al. 2015).

Introducing an ocean acidification effect on juvenile tuna in SEAPODYM

The impact of acidification on the life history of tuna was incorporated by adding a 3rd dimension (an acidification effect) to the natural mortality curve. In this case, the mortality increases with increasing acidity (Figure 1). The parameterisation of the functional response to pH level is based on the experimental study described in Frommel et al. (2016). In the Frommel et al. study (2016), the decrease in pH level was found to significantly reduce larval survival by 64% and 70% at pH 7.3 and 6.9 respectively during the first 7 days. For higher pH levels there are statistically insignificant results with a mean reduction of survival at pH = 7.6 by 27% (mean reduction of 27% with a range of 6% increase down to 49% decrease). It is therefore assumed that additional mortality due to pH is effectively null when pH is above this value.

According to these findings, the monthly mortality rates of larvae in SEAPODYM were increased with decreasing pH as shown on Figure 1. It is assumed that the survival rates observed after 7 days in laboratory experiments under different pH conditions are constant over the 1st month of development, i.e., during the SEAPODYM larval stage. This seems a conservative assumption since the impact can be expected to decrease with size/age. Then, an additional monthly mortality coefficient (Figure 1) related to pH is derived from the observed reduction in survival rate due to pH conditions. For instance, a 70% decrease in larvae survival at pH 6.9 results in an additional monthly mortality coefficient of 1.2.

Three scenarios are tested with different shapes of the functional relationship to take into account the uncertainty of acidification impact at higher pH levels. The scenarios are based on the mortality rates estimated at three different pH values by Frommel et al. (2016), taking into account that at pH 7.6 the result is statistically insignificant:

- S1 (solid line in Fig. 1) – the mean scenario based on the three mean values of mortality observed in the experimental study;
- S2 (dashed curve on Fig. 1) – a high sensitivity scenario to ocean acidification, also implying that pH could have already have an impact in the Eastern Pacific equatorial zone where pH values below 8.0 are regularly observed (Bromhead et al., 2015); and
- S3 (dotted line on Fig. 3) – a low sensitivity scenario to ocean acidification with the lowest reduction at pH 7.6.

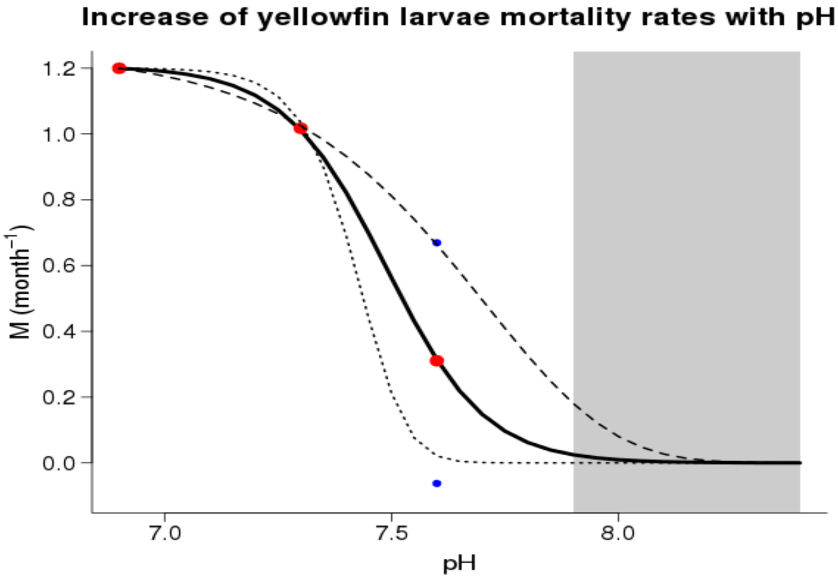

Figure 1: Change in additional monthly mortality rates of yellowfin larvae deduced from experimental results (Frommel et al., 2016) corresponding to 70%, 64% and 27% (red points) decrease in larvae survival during first 7 days of life at pH value of 6.9, 7.3, 7.6 respectively. The solid line shows the analytical function implemented in SEAPODYM to take into account the impact of acidification with these three mean values (scenario S1). Two other curves (dashed, S2 and dotted, S3) are high and low sensitivity scenarios to take into account uncertainty at higher levels of pH. The shaded area corresponds to the historical pH values in the ocean.

Results

Reference simulation from historical hindcast (1980-2010)

The last reference SEAPODYM solution for Pacific yellowfin tuna was presented at the 11th Scientific Committee of the WCPFC (Senina et al. 2015) and revised in 2016 (Nicol et al. 2016). The first solution (NPI-1) was obtained with optimization of the model based on incomplete historical geo-referenced fishing data (1980-2010), representing between 60-75% of the total landings during the last two decades. The revised reference solution (NPI-2), reported for the first time in this paper, was achieved with the full catch-and-effort dataset being raised to the total nominal catch. Another major difference from NPI-1 was the implementation of a Holling-III prey function, and the implementation of a local response to predator (micronekton) density to replace the prey/predator ratio used in the previous definition of the spawning habitat (see Figure 2).

The NPI-2 solution is characterized by changes in the thermal habitats both for spawning and feeding (Table 2, Figure 2). The result in larval distribution is a stronger contrast between areas with less dense concentrations in the central equatorial region, but higher densities in the eastern and western regions (Figure 3). Note that in the optimization with the updated fishing data the primary production series were replaced by satellite-derived variables (1998-2010) in order to fit the huge catches by purse-seine fleets following the strong 1997-1998 ENSO event.

The new thermal habitat of immature and adult fish has a much wider range (32°C to 13.3°C) than in previous estimate (31.5°C - 20.6°C). This is consistent with observations from electronic tagging showing that yellowfin tuna regularly dive in waters below 18°C and in some cases in waters at 12°C ambient temperature (Schaefer et al 2007).

Table 2: Parameter estimates from two model configurations. NPI-1: NEMO-PISCES-INTERIM forcing with incomplete fishing dataset in the likelihood (Senina et al., 2015); and, NPI-2: complete fishing dataset and same forcing as NPI-1 prior to 1998 but satellite PP and respective micronekton fields after. Parameter with [or] were estimated at their lower or upper boundary correspondingly. The dash indicates that the parameter is not effective and could not be estimated.

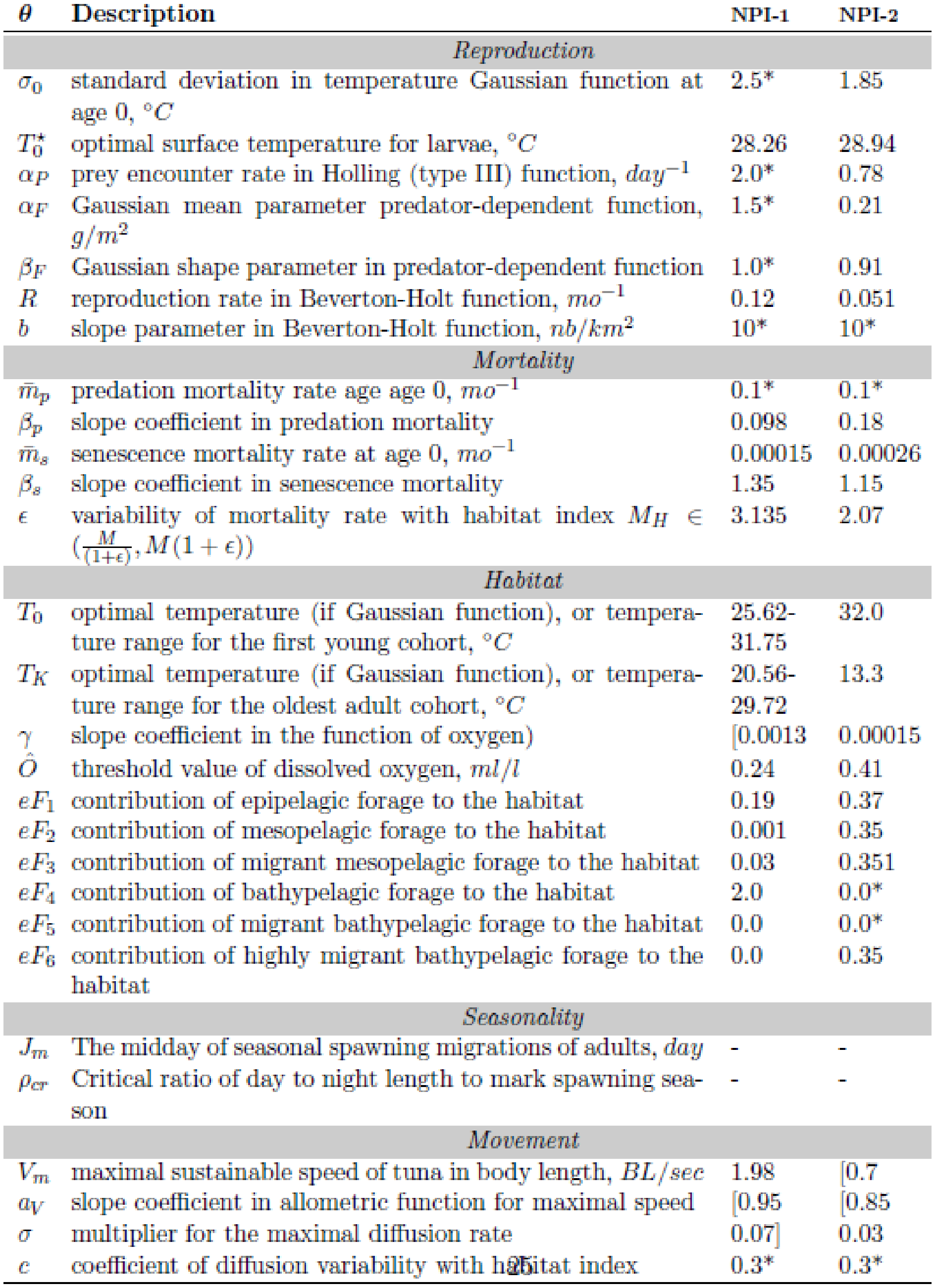

θ	Description	NPI-1	NPI-2
	Reproduction		
σ_0	standard deviation in temperature Gaussian function at age 0, $°C$	2.5*	1.85
T_0^*	optimal surface temperature for larvae, $°C$	28.26	28.94
α_P	prey encounter rate in Holling (type III) function, day^{-1}	2.0*	0.78
α_F	Gaussian mean parameter predator-dependent function, g/m^2	1.5*	0.21
β_F	Gaussian shape parameter in predator-dependent function	1.0*	0.91
R	reproduction rate in Beverton-Holt function, mo^{-1}	0.12	0.051
b	slope parameter in Beverton-Holt function, nb/km^2	10*	10*
	Mortality		
$\bar{m}_p$	predation mortality rate age age 0, mo^{-1}	0.1*	0.1*
β_p	slope coefficient in predation mortality	0.098	0.18
$\bar{m}_s$	senescence mortality rate at age 0, mo^{-1}	0.00015	0.00026
β_s	slope coefficient in senescence mortality	1.35	1.15
ϵ	variability of mortality rate with habitat index $M_H \in (\frac{M}{(1+\epsilon)}, M(1+\epsilon))$	3.135	2.07
	Habitat		
T_0	optimal temperature (if Gaussian function), or temperature range for the first young cohort, $°C$	25.62-31.75	32.0
T_K	optimal temperature (if Gaussian function), or temperature range for the oldest adult cohort, $°C$	20.56-29.72	13.3
γ	slope coefficient in the function of oxygen)	[0.0013	0.00015
$\hat{O}$	threshold value of dissolved oxygen, ml/l	0.24	0.41
eF_1	contribution of epipelagic forage to the habitat	0.19	0.37
eF_2	contribution of mesopelagic forage to the habitat	0.001	0.35
eF_3	contribution of migrant mesopelagic forage to the habitat	0.03	0.351
eF_4	contribution of bathypelagic forage to the habitat	2.0	0.0*
eF_5	contribution of migrant bathypelagic forage to the habitat	0.0	0.0*
eF_6	contribution of highly migrant bathypelagic forage to the habitat	0.0	0.35
	Seasonality		
J_m	The midday of seasonal spawning migrations of adults, day	-	-
ρ_{cr}	Critical ratio of day to night length to mark spawning season	-	-
	Movement		
V_m	maximal sustainable speed of tuna in body length, BL/sec	1.98	[0.7
a_V	slope coefficient in allometric function for maximal speed	[0.95	[0.85
σ	multiplier for the maximal diffusion rate	0.07]	0.03
c	coefficient of diffusion variability with habitat index	0.3*	0.3*

The new reference solution NPI-2 provides a better fit to catch data (Appendix A1). The comparison with MULTIFAN-CL estimate by region (Appendix A2) shows major differences in region 2 where the previous biomass estimate is divided by a factor 10 and much smaller than the MULTIFAN-CL estimate. The biomass is divided by two in region 6 but still remains above the MULTIFAN-CL estimate and there is a smaller decrease in regions 7 and 4. In the main fishing ground areas 3 and 4 of the WCPO, the two models provide close solutions. In region 7, the two models are quite close also if we omit the peak of biomass predicted in 2001 by MULTIFAN-CL. This discrepancy has been investigated and it appears that the biogeochemical model did not predict a strong enough increase in primary production during this period in the eastern-central equatorial Pacific. When replacing the primary production from the biogeochemical model by the satellite derived primary production the peak of biomass is much better reproduced (Appendix A3).

The predicted impact of fishing is readily visible by comparison of simulations with and without fishing mortality (Fig. 3 and A4). The fishing impact is particularly strong on the adult population with a biomass reduced to 40% or less than 30% of the unfished biomass in the EPO and the western equatorial fishing grounds.

This new reference solution NPI-2 provides the initial population conditions and model parameterization for the climate change projections.

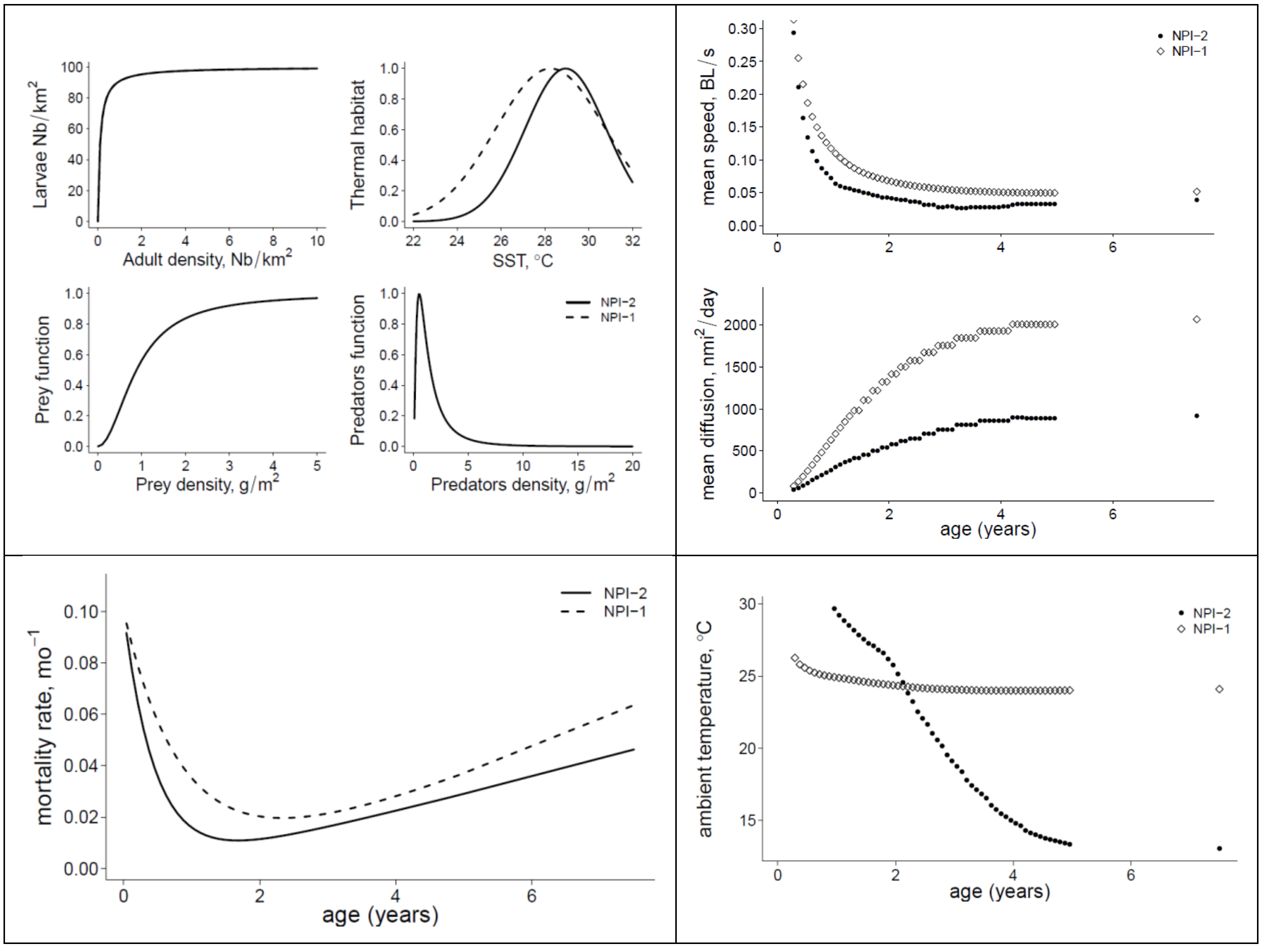

Figure 2: Estimated parameters in the optimization experiments NPI-1 and NPI-2. Evolution of main model parameters through population life history: top left – Spawning habitat and stock recruitment functions, bottom left: mortality function, top right: mean speed at age and diffusion rate at age, bottom right: change in optimal temperature with age (size) for feeding habitat.

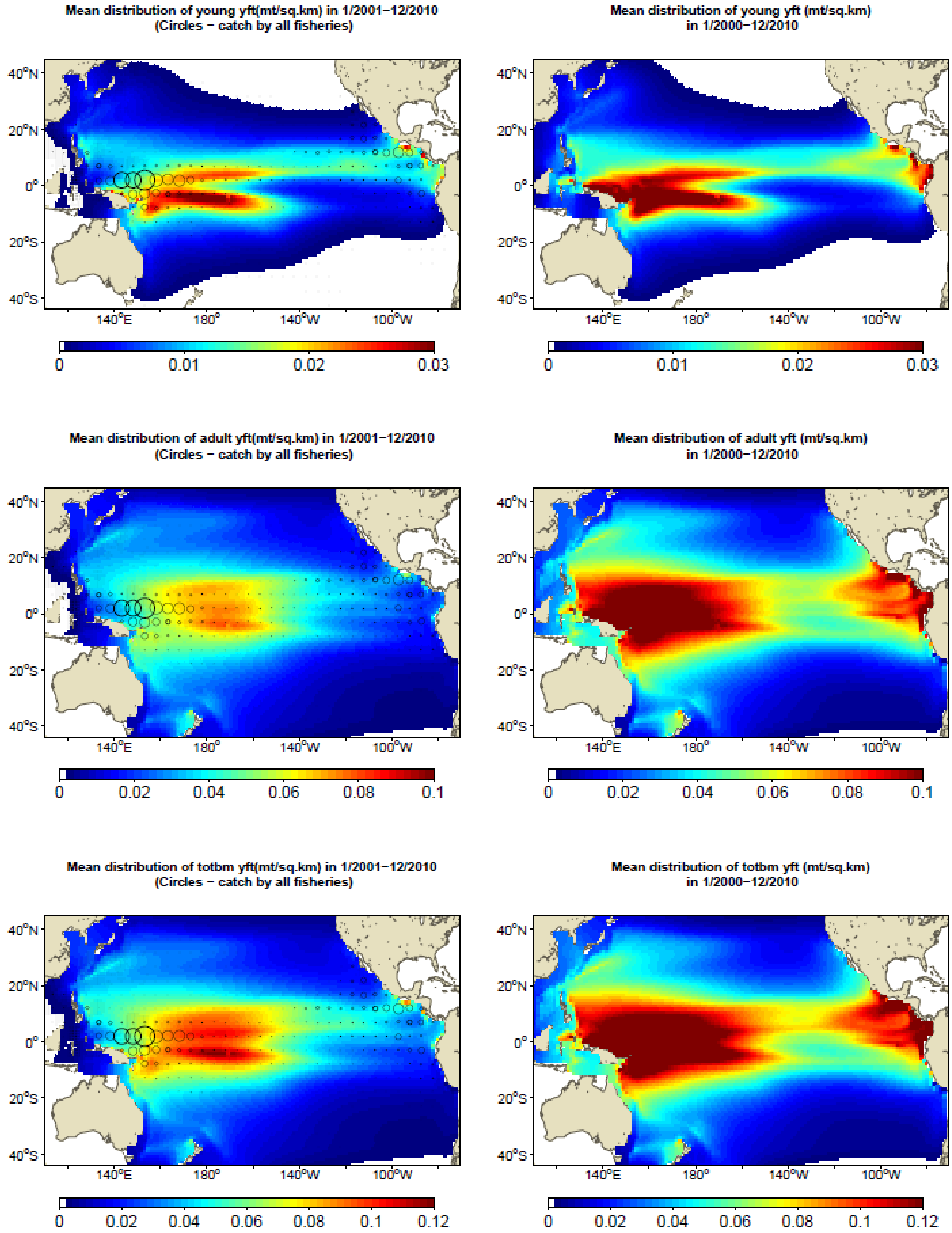
Mean distribution of young yft(mt/sq.km) in 1/2001−12/2010
(Circles − catch by all fisheries)

Mean distribution of young yft (mt/sq.km)
in 1/2000−12/2010

Mean distribution of adult yft(mt/sq.km) in 1/2001−12/2010
(Circles − catch by all fisheries)

Mean distribution of adult yft (mt/sq.km)
in 1/2000−12/2010

Mean distribution of totbm yft(mt/sq.km) in 1/2001−12/2010
(Circles − catch by all fisheries)

Mean distribution of totbm yft (mt/sq.km)
in 1/2000−12/2010

Figure 3: Yellowfin average spatial distributions of (from top to bottom) young, adult and total biomass with (left) and without (right) fishing predicted with revised NPI-2 solution.

Projection of climate change effects under scenario RCP8.5

The well-established approach to deal with uncertainty between models is to run a multi-model ensemble simulation, providing a mean trend with a quantified range of uncertainty. Projections based on the five selected Earth Climate models atmospheric forcings were computed using the same initial conditions and parameterization obtained from the reference historical solution, NPI-2. In addition, for each Earth Climate model forcing three other simulations (S1, S2 and S3, as described in the methods) including a potential pH effect on larval mortality were produced. Therefore, a total of 20 different runs compose the ensemble simulation. As only the impact of climate change is investigated here, the simulations do not include any projection of fishing effort.

The predicted impact of climate change on this yellowfin tuna population is mainly driven by the change in the spawning habitat and subsequent larval recruitment. The projections achieved with the five initial simulations, without including the ocean acidification effect, show average anomalies increasing with time over the century and with opposite direction between the EPO and the WCPO (Figure 4). Decreases in larval recruitment in the WCPO and increases in the EPO are driven by changes in temperature and productivity (prey of larvae).

The additional impact of ocean acidification is minor. There is no discernible impact when considering the low sensitivity scenario (S3). Very small effects (>5%) appear by the end of the century in the eastern equatorial Pacific ocean with the intermediate scenario S1 (Figure 5). The high sensitivity scenario (S2) shows a stronger negative impact on larval recruitment in the same area, with anomalies reaching locally -10% in 2050 and -15% in 2100. Interestingly it shows also a visible but small impact currently for the end of the historical period.

The temporal trends in larval biomass predicted by all simulations are relatively stable in the WCPO until 2050 (Figure 6), and start to decrease in the second half of the century, while the range of model responses widens after the 2060s. In the EPO, there is no clear temporal trend, but the range of cumulated variability from all models is about two times the range simulated over the historical period (Figure 6).

The resulting change in total biomass is presented with the average and its envelope bounded by the 5% and 95% quantile values of the 20 runs of the ensemble simulation (Figure 7). In the WCPO, three periods can be isolated. Until 2050, there is no detectable impact outside of natural variability. After a rapid shift around 2050, a second regime of lower productivity is maintained until 2080. Finally, the end of the time series is marked by one more decline in productivity with a wider range of uncertainty. In the EPO, the higher variability simulated by the climate projections produce higher average total biomass than during the historical period (without fishing). There is a long term trend slightly increasing until the end of the 2070s before stabilization and possibly the beginning of a decreasing tendency (Figure 7).

The variability of predicted changes in unfished biomass by large oceanic region and each model forcing are illustrated in Tables 3 and 4 for the middle and the end of the century. The minimum and maximum values of all simulations for a given model are provided for four oceanic regions, in the western (WTPO), central (CTPO) and eastern (ETPO) tropical Pacific, and the north subtropical Pacific (NPO). In 2050, the most obvious changes relative to the first decade of the century are a large increase of unfished biomass in the ETPO (+37% on average) and a moderate decrease in the WTPO (-14% on average). The main contributions to these changes are the MIROC, MPI and IPSL model forcings for EPO and IPSL, GFDL and NorESM for the WTPO. By the end of the century, the change in the EPO (average +30%) is mainly due to the MPI, NorESM and MIROC forcings, and in the WTPO (average -40%) it is due to the IPSL, MIROC and GFDL forcings. A substantial decrease in unfished biomass is also observed in the central region CTPO (average -29%) driven by the models MIROC IPSL and GFDL. At least for the period selected over the time series and these regions, the mean trend depends on different combinations of model tendencies. There is not one single or couple of models dominating the average trends, nor are trends observed with any model changing in parallel with another over time.

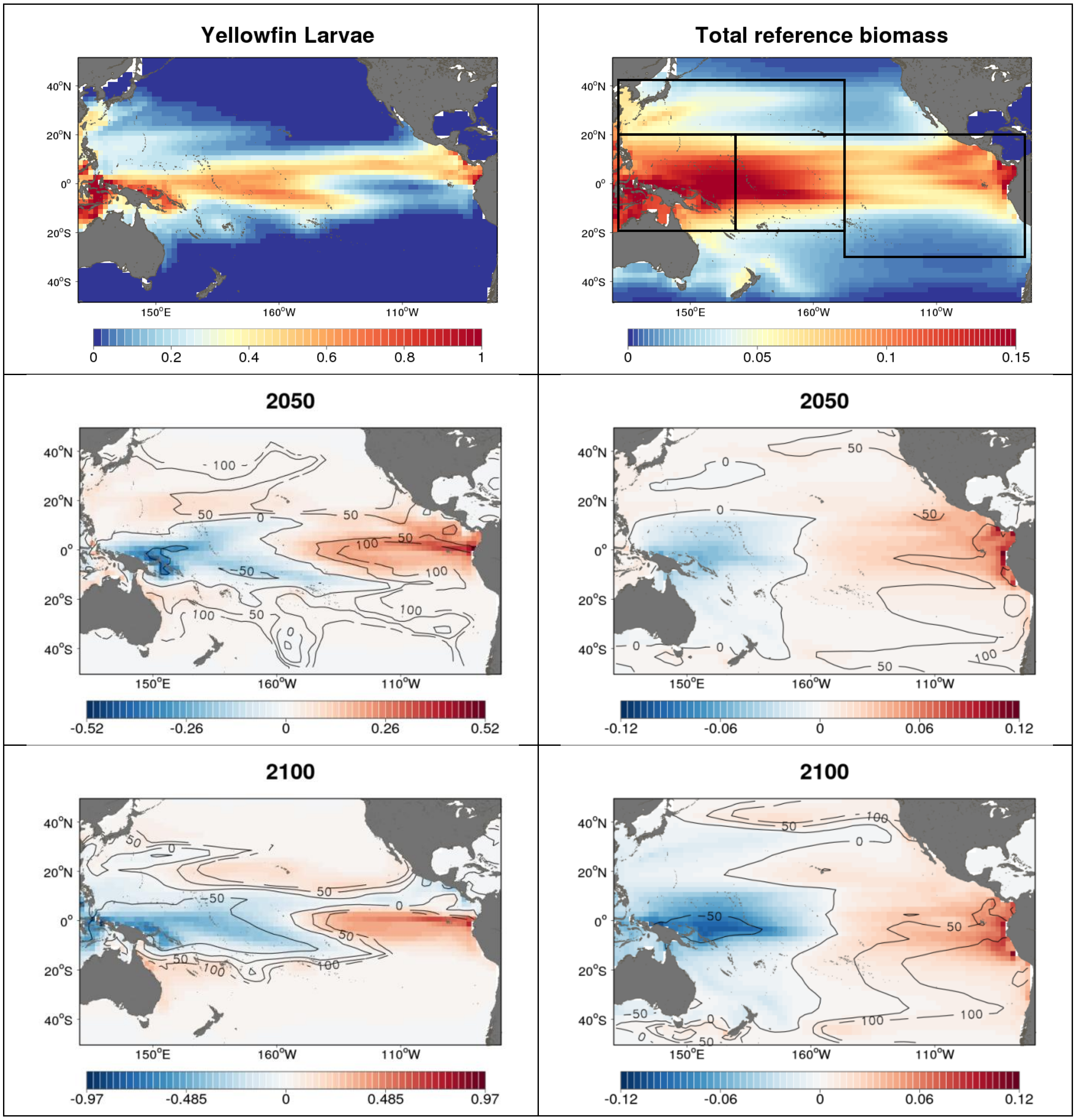

Figure 4: Maps of average distribution from the ensemble simulation of (top-left) yellowfin larvae in Nb/sq. km and (top-right) total virgin (without fishing) biomass (top-right) in mt/sq.km predicted by SEAPODYM in 2001-10. The colour maps for 2050 (2046-55) and 2100 (2090-99) show the average biomass change since 2005 (in respective density units) projected to occur under the high emissions scenario RCP8.5. Isopleths gives the relative percentage change in biomass with respect to 2005, i.e. $100*(B_{year} – B_{REF})/B_{REF}$. Black rectangles show the oceanic regions used in Tables 3 and 4.

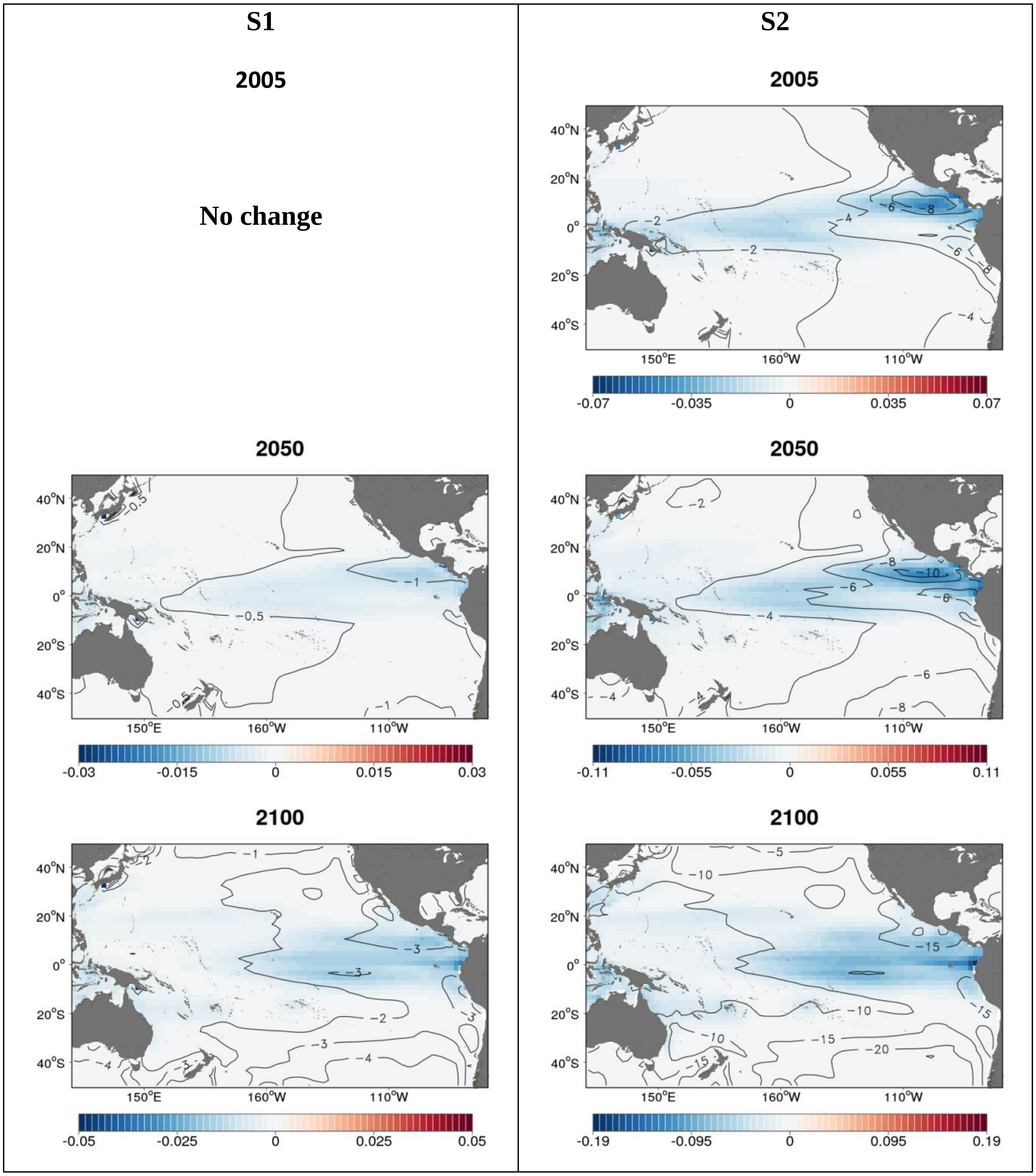

Figure 5: Change in yellowfin larval density due to ocean acidification effects included in SEAPODYM, in 2050 (average 2046-2055) and 2100 (average 2090-2099) for intermediate scenario S1 and high sensitivity scenario S2. There is no change for scenario S3. The colour maps show the average biomass change since 2005 projected to occur under a high emissions scenario (RCP8.5) with 5 different atmospheric forcings generated by Earth Climate models. Isopleths gives the relative percentage change in biomass with respect to 2005, i.e. 100*(B_{year} – B_{REF})/B_{REF}.

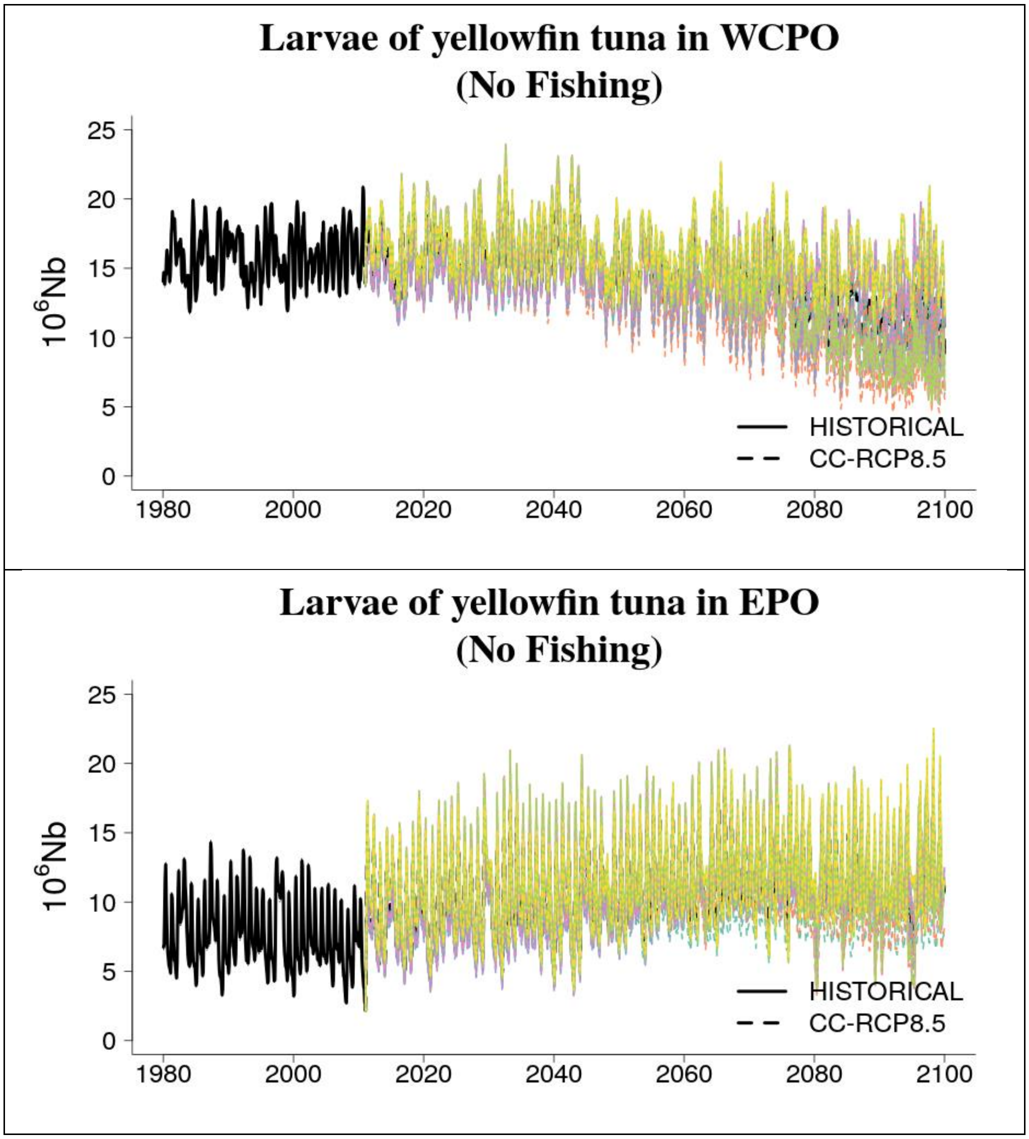

Figure 6: Envelope of predictions computed from 20 runs, including five runs without the impact of pH during the CC period, and, three runs per model corresponding to S1, S2 and S3 scenarios of ocean acidification impact. Top panel is WCPO, bottom panel is EPO.

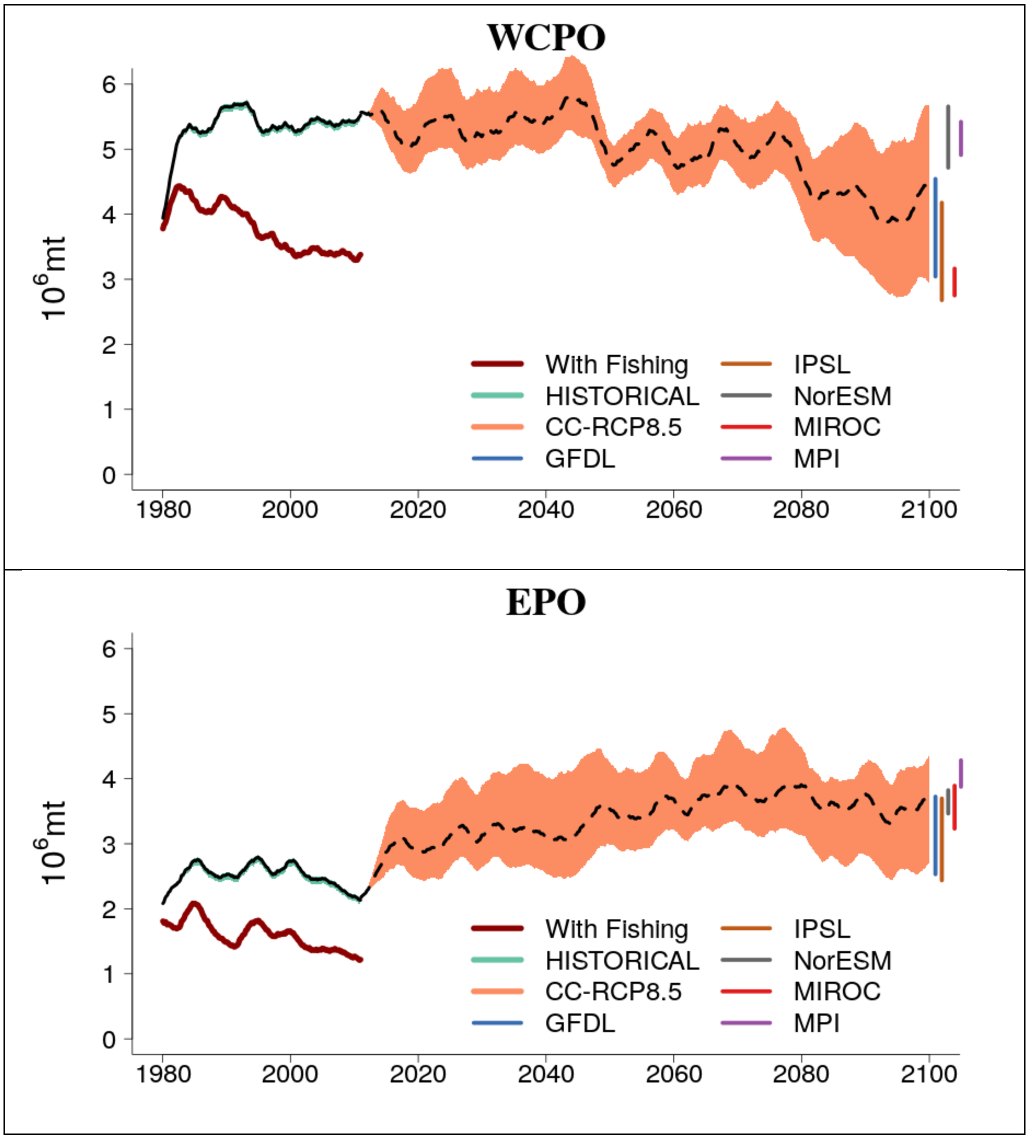

Figure 7: Envelope of predictions computed from an ensemble simulation composed of 20 runs, including five runs without the impact of pH during CC period and three runs per model corresponding to S1, S2 and S3 scenarios of ocean acidification impact. The dashed line is the mean of the ensemble and the envelope is defined by the 5% and 95% quantile values of the 20 runs. The ranges by model forcing for the last 10 years (2090-2100) are shown with the colour bars at the end of the time series.

Table 3: Projected changes (in percentages of reference unfished biomass) predicted for yellowfin tuna stock in 2050 (average over January 2046 – December 2055) from the ensemble simulation (20 runs) for Pacific regions. The reference biomass average was computed over the period January 2001 – December 2010. Region boundaries: NPO = 120°E-150°W and 40°N-20°N; WTPO = 120°E - 170°E and 20°N-20°S; CTPO = 120°E - 170°E and 20°N-20°S; EPO = 150°W-70°W and 30°N-20°S.

Region	**GFDL**		**IPSL**		**NorESM**		**MIROC**		**MPI**		**All**
	$\underline{\delta B}$	$\overline{\delta B}$	$\underline{\delta B}$	$\overline{\delta B}$	$\underline{\delta B}$	$\overline{\delta B}$	$\underline{\delta B}$	$\overline{\delta B}$	$\underline{\delta B}$	$\overline{\delta B}$	
NPO	-1	5	6	13	7	9	13	15	6	8	**6**
WTPO	-17	-12	-23	-18	-13	-12	-11	-9	-8	-7	**-14**
CTPO	-13	-6	-9	-2	-18	-16	3	6	1	4	**-7**
EPO	17	29	30	45	21	26	68	75	48	54	**37**
Pacific	**-18**		**-14**		**-19**		**-2**		**-7**		**-12**

Table 4: Projected changes (in percentages of reference unfished biomass) predicted for yellowfin tuna stock in 2100 (average over January 2091 – December 2100) from the ensemble simulation (20 runs) for Pacific regions. The reference biomass average was computed over the period January 2001 – December 2010. Region boundaries: NPO = 120°E-150°W and 40°N-20°N; WTPO = 120°E - 170°E and 20°N-20°S; CTPO = 120°E - 170°E and 20°N-20°S; EPO = 150°W-70°W and 30°N-20°S.

Region	**GFDL**		**IPSL**		**NorESM**		**MIROC**		**MPI**		**All**
	$\underline{\delta B}$	$\overline{\delta B}$	$\underline{\delta B}$	$\overline{\delta B}$	$\underline{\delta B}$	$\overline{\delta B}$	$\underline{\delta B}$	$\overline{\delta B}$	$\underline{\delta B}$	$\overline{\delta B}$	
NPO	-33	-13	-24	-2	19	21	-34	-32	3	5	**-14**
WPO	-48	-34	-61	-50	-19	-17	-54	-53	-18	-16	**-40**
CPO	-40	-21	-46	-29	-11	-9	-50	-49	3	6	**-29**
EPO	6	45	1	38	45	51	34	40	65	72	**30**
Pacific	**-28**		**-35**		**-12**		**-37**		**-5**		**-23**

Discussion

While the ocean is warming, it is also absorbing about a quarter of the anthropogenic CO2 released into the atmosphere, changing the chemistry of the sea water to more acidic conditions. These changes start to have consequences on organisms and ecosystems (Hoegh-Guldberg et al., 2014; Pörtner et al., 2014) in terms of habitats and species distributions, trophic network reorganization, and biodiversity (invasive species and species extinction). Together with intensive fishing, these changes will challenge the global tuna industry and the existing international agreements needed to manage highly migratory pelagic species such as tuna, as well as the economy and food security of many small Pacific Island Countries (Bell et al. 2013; 2017; Gilman et al 2016). Therefore, despite large uncertainties about the future state of the oceans, it is crucial to explore the potential impact that climate warming and ocean acidification may have on tuna populations, and then, to integrate these results into a precautionary approach for the sustainable exploitation of these stocks.

SEAPODYM is a useful modelling framework to investigate the impact of climate changes on tuna populations. It integrates key relationships between fish population dynamics and the environmental conditions of their marine ecosystem in a spatially explicit representation, with a robust estimation approach of population dynamics and fisheries parameters. In previous modelling studies, the IPCC climate change AR4-A2 scenario ("business as usual") was used with this model to project the future of different Pacific tuna populations (Lehodey et al 2010, 2013, 2015; Bell et al. 2013). However, the potential for ocean acidification impact was not included as very little knowledge was available to model the effect on tuna biology and thus population dynamics. Recent experimental studies on yellowfin tuna (Bromhead et al. 2015; Frommel et al. 2016) have provided the first information making this tractable. The information from those studies have been used in this research to introduce potential impacts of ocean acidification on the most critical stage (larvae) of the fish life cycle.

The simulation results suggest a weak impact, even with the highest sensitivity scenario. This could be expected however, from the relationship to the pH deduced from the laboratory experiments and the projected change in pH. By the end of the century, pH at the surface ocean in the tropics is projected to decrease from preindustrial levels of 8.17 to 7.77. At this lower level, the detected impact on yellowfin tuna larvae reared in laboratory is still weak and only the high sensitivity scenario in the model starts to introduce additional mortality on larvae due to pH. With longer time scale projections, and predicted lower pH values, e.g. a decrease to 7.5 or lower in 2300 (Hartin et al 2016; Frommel et al. 2016), a much more critical impact on larval mortality would be expected. An interesting result from this study is the possibility that there could be already a small pH effect on larval mortality in the eastern equatorial Pacific with the high sensitivity scenario. If it is the case, it could be estimated directly through optimisation experiments. However in absence of a large dataset to inform the model on the variability of larvae and small juvenile stages, the model will be likely be insufficiently sensitive to estimate the parameters of the functional relationship with pH.

On long-term scales it would be necessary to explore also some genetic capacity to adapt (Munday et al 2013). The speed at which adaptation is likely to occur in tuna is not known. There might exist already part of the population already more acclimated to lower pH, as in the EPO where there is a greater natural variation in pCO_2 and acidity levels than in the WCPO. Such plasticity has been observed in arctic zooplankton where the sensitivity to acidification is correlated with natural exposures to different pCO2 ranges (Lewis et al. 2013). Adaptation due to epigenetic mechanisms under environmental influence could also be expected and in that case, change at a much faster rate (Feil and Fraga 2012). While laboratory and genetic studies can help to determine the rate and scope of adaptation, it is already possible to test sensitivity analyses, with simulations allowing parameters to shift through time (e.g. Lehodey et al. 2015), e.g. toward a higher tolerance to lower pH. Further developments combining both laboratory experiments and modelling should explore the potential of synergistic effects of temperature and pH changes, with a range of plausible scenarios, including the possibility that sensitivity of metabolism to pH disturbance could induce a narrowing of thermal tolerance windows (Pörtner 2008).

We suggest that simulations testing genetic adaptation and synergistic effects should become new runs in the ensemble simulation. The ensemble could be also enlarged with projections achieved with other coupled physical biogeochemical models, to account for uncertainties associated to these models in addition to those generated by the atmospheric forcing. Given the exponential increase in computational time that this type of exercise represents, it is extremely helpful to use a reference set of atmospheric forcings as those produced for this analysis with bias corrections based on historical atmospheric reanalysis. This approach should be proposed as a standard to facilitate the use of IPCC model projections outputs.

The approach developed in this study provides a general framework to investigate the future of tuna populations under the impact of climate change. However, it remains to apply fishing impact. The major external driver of the tuna population dynamics since the 20th century remains the industrial exploitation by fisheries. This impact has been included and estimated in the reference model and future projections based on IPCC scenarios should also include a range of fishing scenarios. Some simple scenarios can be proposed as the mean fishing effort observed over recent years, but the result would likely be biased due to the change in distribution of the resource that will likely also drive changes in fishing effort distribution. A more robust option is to assume that catch will be removed proportionally to the fish biomass density; however this assumes constant catchability over time and space. Another option is to define a maximum allowed catch, at either basin scale or for sub-regions that could be dynamically linked to some simple rules (e.g., maintaining 40% of spawning biomass). Alternative scenarios could be proposed and the Scientific Committee of the WCPFC is an ideal place for starting such a discussion.

Acknowledgements and Donors

This project (WCPFC Project 62) is currently supported by Secretariat of the Pacific Community, Collecte Localisation Satellites, and Institut de Recherche pour le Développement with financial assistance from the Australian Government Overseas Aid Program (AUSAID), the GEF OFMP II Project, the New Zealand Ministry of Foreign Affairs and Trade, and the Government of Monaco. The Inter American Tropical Tuna Commission has provided access to non-public domain data for the purposes of implementing the work programme of the WCPFC SC, and the WCPFC project 62 in particular. We are grateful to Peter Williams and Sylvain Caillot for their support in processing fishing and tagging data.

References

Aumont O., Ethé C., Tagliabue A., Bopp L., Gehlen M., 2015. PISCES-v2: an ocean biogeochemical model for carbon and ecosystem studies. *Geosci. Model Dev*., 8, 2465–2513.

Barnett TP, Pierce DW, Achuta Rao KM, Gleckler PJ, Santer BD, Gregory JM, Washington WM (2005) Penetration of human-induced warming into the world‘s oceans. Science 309:284–287.

Baumann H, Talmage SC, Gobler CJ (2012) Reduced early life growth and survival in a fish indirect response to increased carbon dioxide. Nature Clim. Change 2:38–41.

Bell J.D., Cisneros A., Crowder L, Hanich Q., Johnson J., Lehodey P., Moore B., Pratchett M., Reygondeau G., Senina I., Vidrin J., Warbnitz C., (2017) Adaptations to maintain the contributions of small-scale fisheries to food security in the Pacific Islands. Marine Policy, http://dx.doi.org/10.1016/j.marpol.2017.05.019

Bell JD, Ganachaud A., Gehrke PC, Griffiths SP, Hobday AJ, Hoegh-Guldberg O, Johnson, JE Le Borgne R, Lehodey P, Lough JM, Matear RJ, Pickering TD, Pratchett MS, Sen Gupta A, Senina I and Waycott M., (2013) Tropical Pacific fisheries and aquaculture will respond differently to climate change. *Nature Climate Change,* 3: 591–599.

Bellenger H., Guilyardi E., Leloup J., Lengaigne M., Vialard J. 2014. ENSO representation in climate models: from CMIP3 to CMIP5. Climate Dynamics (42) 7–8: 1999–2018.

Bromhead D., Scholey V., Nicol S., Margulies D., Wexler J., Stein M., Hoyle S., Lennert-Cody C., Williamson J., Havenhand J., Ilyina T., Lehodey P. (2015). The Potential Impact of Ocean Acidification Upon Eggs and Larvae of Yellowfin Tuna (*Thunnus albacares*). *Deep Sea Research* II, 113: 268–279

Caldeira K, Wickett ME (2003) Anthropogenic carbon and ocean pH. Nature 425:365.

Chambers RC, Candelmo AC, Habeck EA, Poach ME, Wieczorek D, Cooper KR, Greenfield CE, Phelan BA (2014) Effects of elevated CO2 in the early life stages of summer flounder, *Paralichthys dentatus*, and potential consequences of ocean acidification. Biogeosciences 11:1613–1626.

Dee, D.P., Uppala, S.M., Simmons, A.J., Berrisford, P., Poli, P., Kobayashi, S. and 30 authors, 2011. The ERA-Interim reanalysis: configuration and performance of the data assimilation system. *Q. J. R. Meteorol. Soc.*, 137, 553 – 597.

Feely RA, Sabine CL, Lee K, Berelson W, Kleypas J, Fabry VJ, Millero FJ (2004) Impact of anthropogenic CO2 on the CaCO3 system in the oceans. Science 305:362–366.

Feil R, Fraga MF (2012) Epigenetics and the environment: emerging patterns and implications. Nat. Rev. Genet. 13:97-109.

Frommel A., Margulies D., Wexler J. B., Stein M. S., Scholey V. P. Williamson J. E., Bromhead D., Nicol S., Havenhand J. 2016. Ocean acidification has lethal and sub-lethal effects on larval development of yellowfin tuna, *Thunnus albacares*, Journal of Experimentaal Marine Biology and Ecology 482: 18-24.

Gilman, E., Allain, V., Collette, B., Hampton, J., Lehodey, P. (2016). Effects of Ocean Warming on Pelagic Tunas, a Review. Pages 254-270 in: Laffole, D., Baxter, J. (Eds.). Explaining Ocean Warming: Causes, Scale, Effects and Consequences. ISBN 978-8317-1806-4. IUCN – International Union for the Conservation of Nature, Gland, Switzerland.

Hartin, CA., Bond-Lamberty B, Patel P, Mundra A. (2016): Ocean acidification over the next three centuries using a simple global climate carbon-cycle model: projections and sensitivities. Biogeosciences, 13: 4329-4342.

Hoegh-Guldberg O, Cai R, Poloczanska ES, Brewer PG, Sundby S, Hilmi K, Fabry VJ, Jung S. 2014. The ocean. In: Climate Change 2014: Impacts, Adaptation and Vulnerability. Contribution of Working Group II to the Fifth Assessment Report of the Intergovernmental Panel on Climate Change. Field CB, Barros VR, Dokken DJ, Mach KJ, Mastrandrea MD, Bilir TE, Chatterjee M, Ebi KL, Estrada YO, Genova RC, et al. (eds). Cambridge University Press, Cambridge, UK and New York, NY, USA. pp. 1655-1731.

Langley A, Hoyle S, Hampton J (2011). Stock assessment of yellowfin tuna in the western and central Pacific Ocean. 7th Regular session of the Scientifc Committee of the Western Central Pacific Fisheries Commission, Pohnpei, Federated States of Micronesia, 9-17 August 2011. WCPFC-SC7-2011/SA-WP-03 (Rev.1-03Aug2011): 135 pp.

Lehodey P., Senina I., Murtugudde R. (2008). A Spatial Ecosystem And Populations Dynamics Model (SEAPODYM) - Modelling of tuna and tuna-like populations. Progress in Oceanography, 78: 304-318.

Lehodey P, Senina I, Calmettes B, Hampton J, Nicol S (2013) Modelling the impact of climate change on Pacific skipjack tuna population and fisheries. Climatic Change 119:95-109.

Lehodey P., (2004) A Spatial Ecosystem And Populations Dynamics Model (SEAPODYM) for tuna and associated oceanic top-predator species: Part II – Tuna populations and fisheries. 17th meeting of the Standing Committee on Tuna and Billfish, Majuro, Republic of Marshall Islands, 9-18 Aug. 2004, Oceanic Fisheries Programme, Secretariat of the Pacific Community, Noumea, New Caledonia, *Working Paper*: ECO-2: 36 pp. http://www.spc.int/OceanFish/Html/SCTB/SCTB17/ECO-2.pdf

Lehodey P., Chai F., Hampton J. (2003). Modelling climate-related variability of tuna populations from a coupled ocean-biogeochemical-populations dynamics model. *Fisheries Oceanography*, 12(4): 483-494

Lehodey P., Senina I., Calmettes B, Hampton J, Nicol S. (2013). Modelling the impact of climate change on Pacific skipjack tuna population and fisheries. *Climatic Change*, DOI 10.1007/s10584-012-0595-1, 119 (1): 95-109.

Lehodey P., Senina I., Nicol S., Hampton J. (2015). Modelling the impact of climate change on South Pacific albacore tuna. Deep Sea Research. 113: 246–259.

Lehodey P., Senina I., Sibert J., Bopp L, Calmettes B., Hampton J., Murtugudde R. (2010). Preliminary forecasts of population trends for Pacific bigeye tuna under the A2 IPCC scenario. *Progress in Oceanography.* 86: 302–315

Lehodey, P., Hampton, J., Brill, R.W., Nicol, S., Senina, I., Calmettes, B., Pörtner, H.O., Bopp, L., Ilyina,T., Johann D. Bell, and J. Sibert (2011). Vulnerability of oceanic fisheries in the tropical Pacific to climate change. *In* Bell J., Johnson JE, Hobday AJ (Ed.), Vulnerability of Tropical Pacific Fisheries and Aquaculture to Climate Change. Secretariat of the Pacific Community. Noumea New Caledonia. pp. 433-492

Lewis, C.N., Brown, K.A., Edwards, L.A., Cooper, G., Findlay H.S., (2013). Sensitivity to ocean acidification parallels natural pCO_2 gradients experienced by Arctic copepods under winter sea ice. PNAS, 110 (51) pp. E4960-E4967

Miller GM, Kroon FJ, Metcalfe S, Munday PL (2015) Temperature is the evil twin: Effects of increased temperature and ocean acidification on reproduction in a reef fish. Ecol. Appl. 25:603-620.

Murray CS, Malvezzi A, Gobler CJ, Baumann H (2014) Offspring sensitivity to ocean acidification changes seasonally in a coastal marine fish. Mar. Ecol. Prog. Ser. 504:1-11.

Munday P.L., Warner R.R., Monro K., Pandolfi J.M., Marshall D.J. (2013). Predicting evolutionary responses to climate change in the sea. Ecology Letters, 16: 1488–1500

Nicol S, Bromhead D, Frommel A, Gillings M, Gleeson D, Havenhand J, Lehodey P, Margulies D, Moore T., Munday P., Parsons D, Senina I, Smith N, Williamson J. (2016). Predicting the impacts of ocean acidification on pelagic fishes. International workshop on the Impact of Ocean acidification, January 2015, Sydney Australia, 16 pp.

Nicol S, Dessert M, Gorgues T, Aumont O, Menkes C, Lehodey P. Project 62: Progress report on climate simulations. WCPFC, 10th Regular Session of the Scientific Committee, Majuro, Republic of the Marshall Islands, 6-14 August 2014, WCPFC-SC10-2014/EB-IP-02, 13 pp.

Pörtner HO (2008). Ecosystem effects of ocean acidification in times of ocean warming: a physiologist's view. Marine Ecology Progress Series 373: 203-217.

Pörtner HO, Karl DM, Boyd PW, Cheung W, Lluch-Cota S, Nojiri Y, Schmidt DN, Zavialov PO, Alheit J, Aristegui J, Armstrong C, Beaugrand G, Belkovich V, Bowler C, Brewer P, Church M, Cooley SR, del Monte-Luna P, Edwards M, Flint M, Follows MJ, Frölicher T, Fulton EA, Gattuso JP, Hoegh-Guldberg O, Hofmann EE, Knoll AH, Levin LA, Menzel L, Moloney CL, Perry RI, Poloczanska ES, Roberts JM, Rost B, Sarmiento JL, Sedlacek J, Storch D, Wiencke C, Wittmann AC (2014) Ocean Systems. In: Climate Change 2014: Impacts, Adaptation, and Vulnerability. Part A: Global and Sectoral Aspects. Contribution of Working Group II to the Fifth Assessment Report of the Intergovernmental Panel on Climate Change. Pages 411-484. Cambridge University Press.

Schaefer KM., Fuller DW., Block BA. (2007). Movement behaviour, and habitat utilization of yellowfin tuna (*Thunnus albacares*) in the northeastern Pacific Ocean, ascertained though archival tag data. Mar. Biol. 152: 503-525.

Senina I., Lehodey P., Calmettes B., Nicol S., Caillot S., Hampton J. and Williams P. (2015). SEAPODYM application for yellowfin tuna in the Pacific Ocean. 11th Regular Session of the scientific committee, Pohnpei, Federated States of Micronesia, 5-13 August 2015, WCPFC-SC11-2015/EB-IP-01: 66 pp

Senina I., Lehodey P., Calmettes B., Nicol S., Caillot S., Hampton J. and P. Williams (2016). Predicting skipjack tuna dynamics and effects of climate change using SEAPODYM with fishing and tagging data. WCPFC, 12th Regular Session of the Scientific Committee, Bali, Indonesia 3–11 August 2016, WCPFC-SC12-2016/EB WP-01: 71 pp. http://www.wcpfc.int/node/27443

Senina I., Sibert J., Lehodey P. (2008). Parameter estimation for basin-scale ecosystem-linked population models of large pelagic predators: application to skipjack tuna. *Progress in Oceanography*, 78: 319-335.

Supplementary Material

Appendix A1

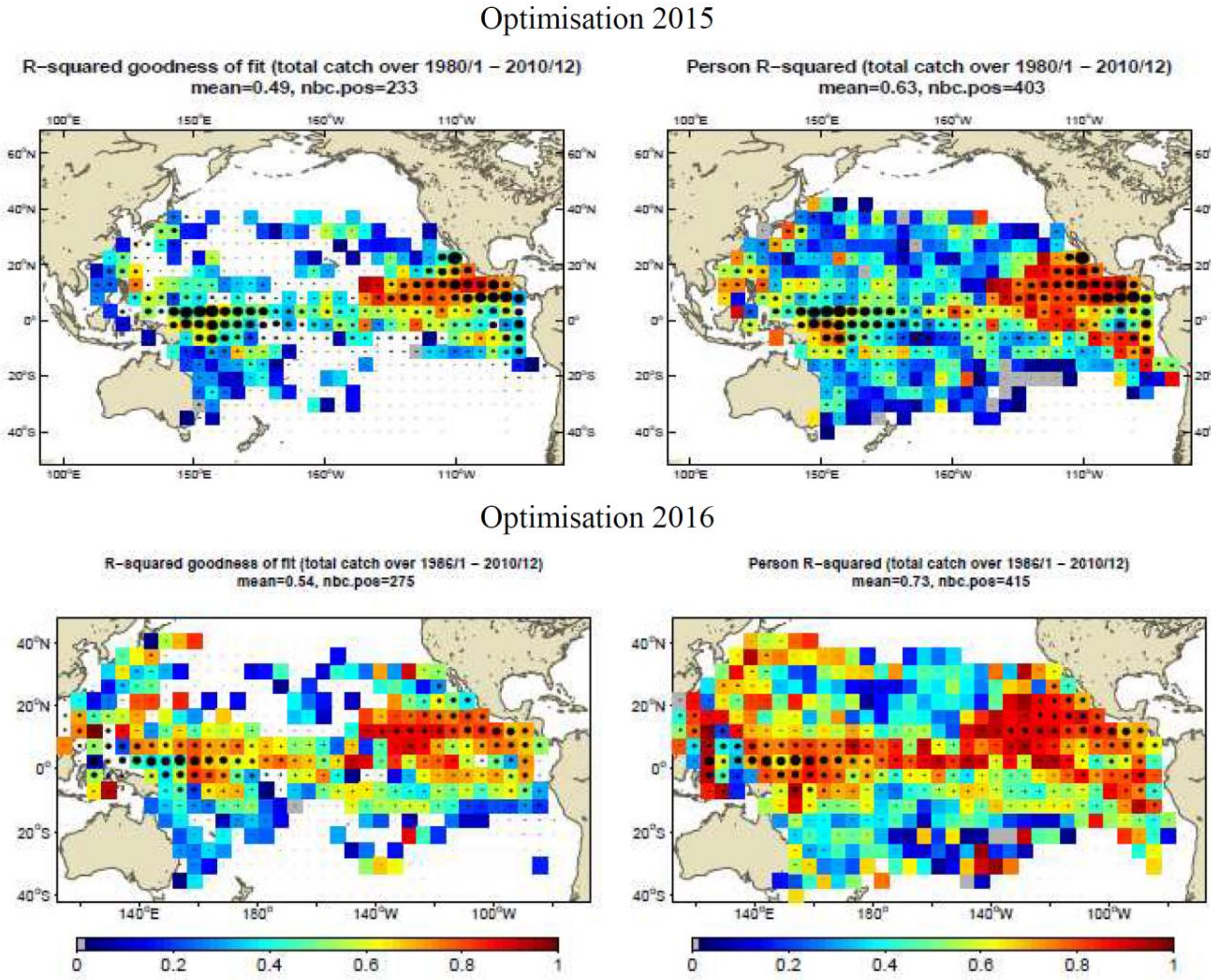

Figure A1: Comparison of spatial maps of validation metrics between two optimization experiments for yellowfin: (left) R-squared goodness of fit and (right) squared Pearson correlation coefficient

Appendix A2

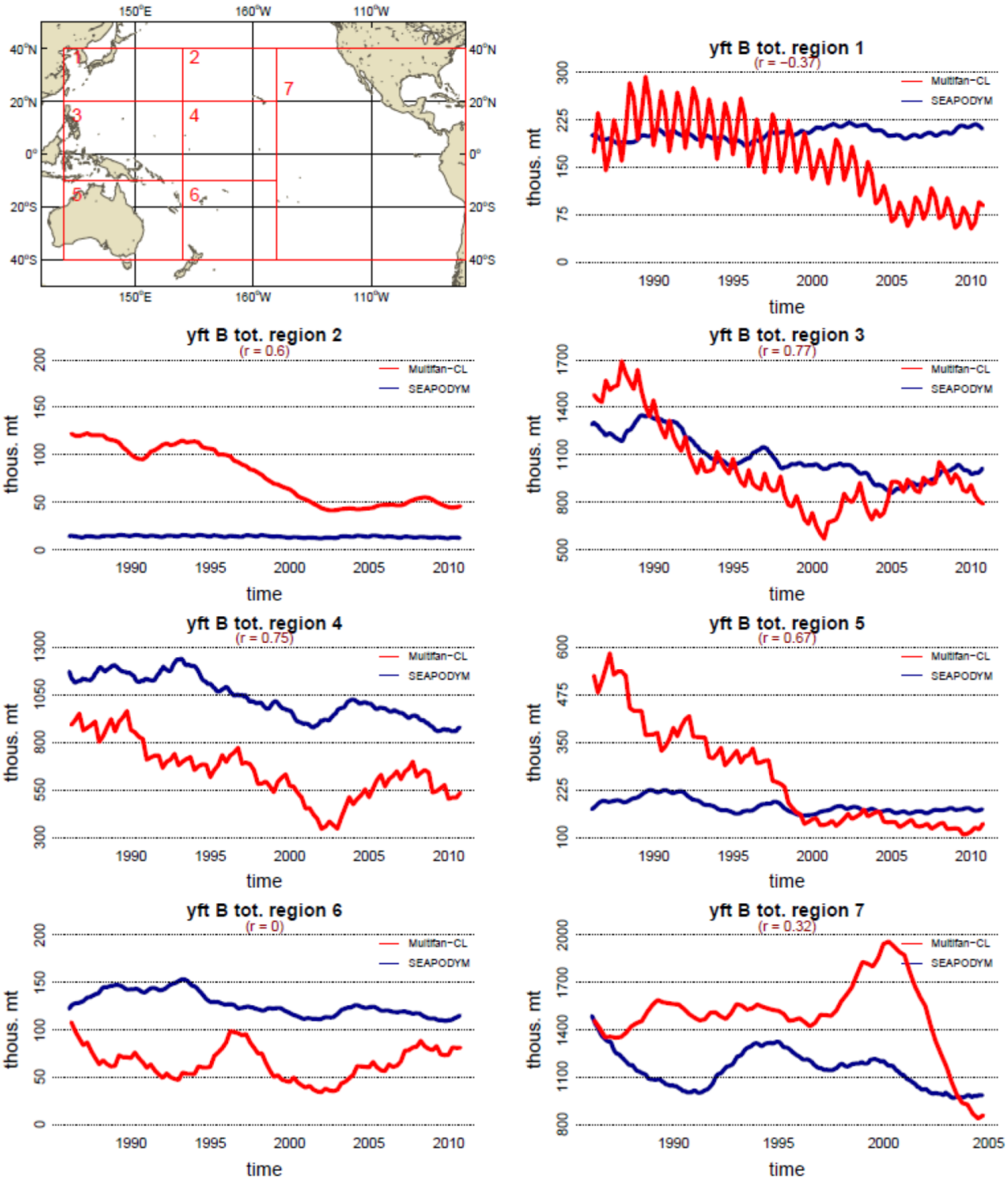

Figure A2: Regional comparison between SEAPODYM and Multifan-CL model predictions for total (immature and mature) biomass with the revised INTERIM optimization

Appendix A3

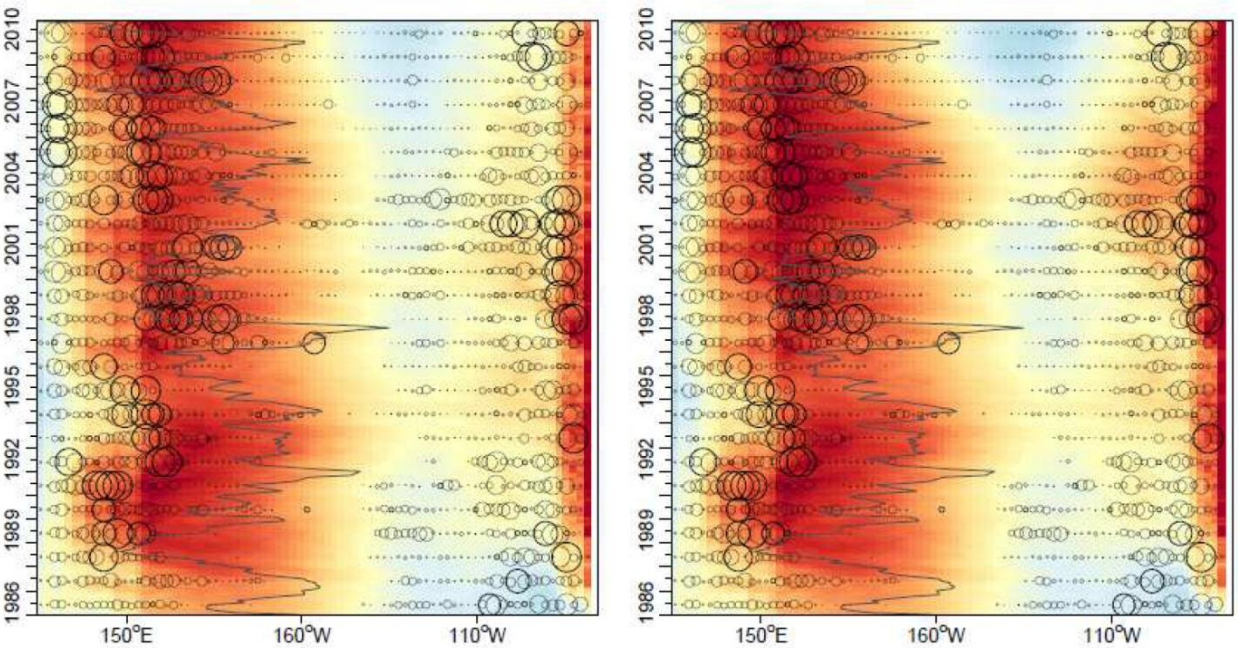

Figure A3: Variability of tropical (average over 10°S-10°N) total biomass of yellowfin tuna with PS catches (proportional to circles) and Southern Oscillation Index. The result from the revised INTERIM optimization (left) is compared to the result (right) with a simulation using satellite derived primary production. Note the peak in biomass predicted in the EPO with satellite primary production in 2001-2004.

Appendix A4

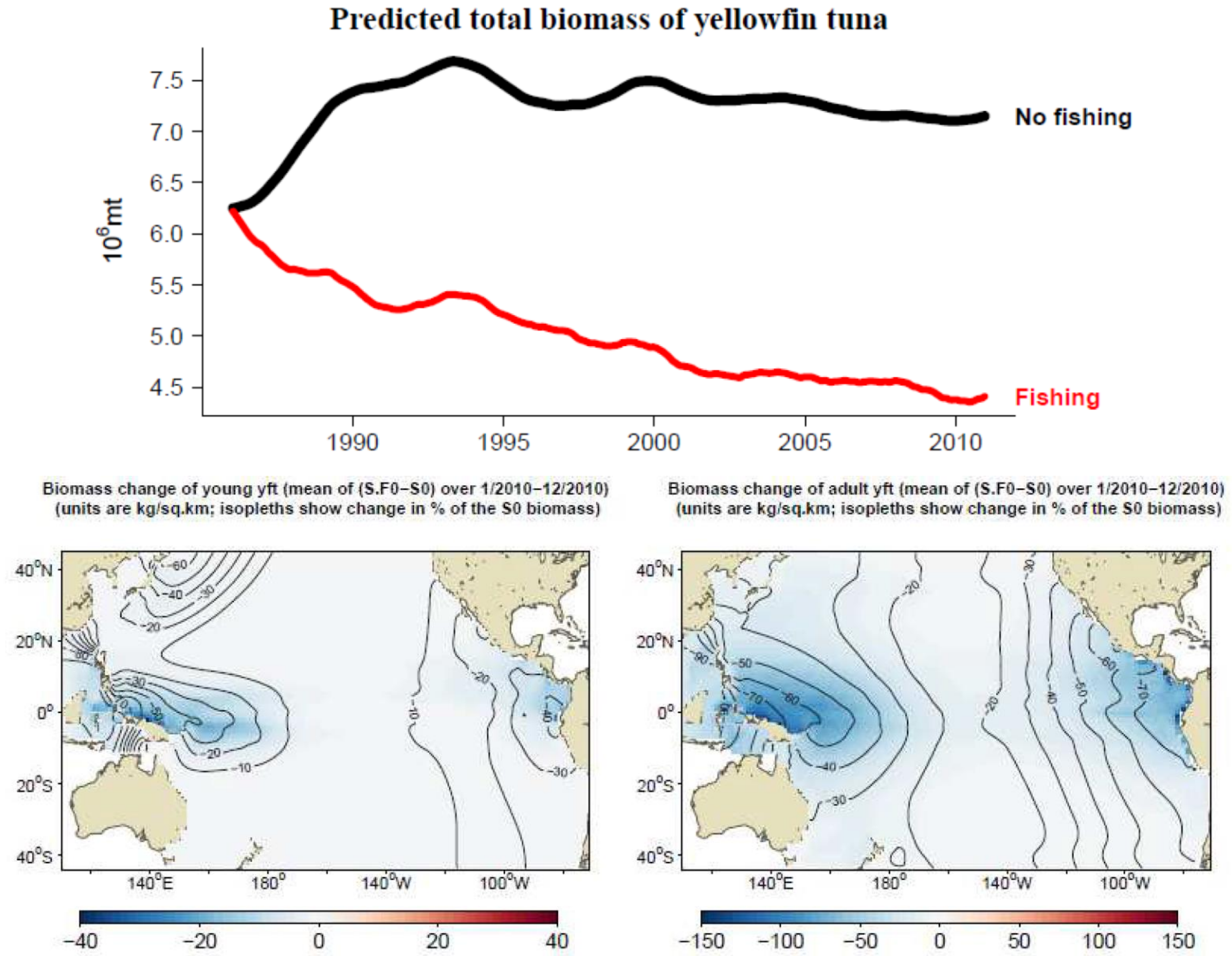

Figure A4: Quantification of the fishing impact of Pacific yellowfin tuna. Spatial fishing impact on young and adult population stages is shown with contour lines of the index (B_{F0}-B_{Ref}) / B_{F0} and color background indicating the average biomass reduction due to fishing (kg /km$_2$).